Multi-scroll hidden attractors and multi-wing hidden attractors in a 5-dimensional memristive system*

Xiaoyu Hu(胡晓宇)†, Chongxin Liu(刘崇新), Ling Liu(刘凌), Yapeng Yao(姚亚鹏), and Guangchao Zheng(郑广超)

State Key Laboratory of Electrical Insulation and Power Equipment, School of Electrical Engineering, Xi'an Jiaotong University, Xi'an 710049, *China*

(Received 24 April 2017; revised manuscript received 1 August 2017; published online 30 September 2017)

A novel 5-dimensional (5D) memristive chaotic system is proposed, in which multi-scroll hidden attractors and multi-wing hidden attractors can be observed on different phase planes. The dynamical system has multiple lines of equilibria or no equilibrium when the system parameters are appropriately selected, and the multi-scroll hidden attractors and multi-wing hidden attractors have nothing to do with the system equilibria. Particularly, the numbers of multi-scroll hidden attractors and multi-wing hidden attractors are sensitive to the transient simulation time and the initial values. Dynamical properties of the system, such as phase plane, time series, frequency spectra, Lyapunov exponent, and Poincaré map, are studied in detail. In addition, a state feedback controller is designed to select multiple hidden attractors within a long enough simulation time. Finally, an electronic circuit is realized in Pspice, and the experimental results are in agreement with the numerical ones.

Keywords: multi-scroll hidden attractors, multi-wing hidden attractors, multiple lines equilibria, no equilibrium

PACS: 05.45.–a, 05.45.Jn, 05.45.Pq **DOI:** 10.1088/1674-1056/26/11/110502

1. Introduction

It is confirmed that dynamical systems with multi-scroll attractors or multi-wing attractors carry much more complexity than those with fewer attractors, and they have been widely used in some areas, such as image encryption,[1] secure communication,[2,3] and chaotic cryptanalysis.[4] Therefore, during the last few decades the dynamical systems with multi-scroll attractors or multi-wing attractors have attracted a great deal of attention from researchers.[5–7] Meanwhile, various nonlinear control schemes which are based on nonlinear functions are proposed to generate multi-scroll attractors or multi-wing attractors, such as hyperbolic function,[8] trigonometric function,[9,10] and switching controller.[11,12] In addition, the study on realization of multi-scroll attractors or multi-wing attractors makes them observable in analog circuits.[13–16] Particularly, in some fractional order systems,[17,18] and memristor-based systems,[19–22] multi-scroll attractors or multi-wing attractors can also be obtained.

The hidden attractor[23–25] is a hot topic and has attracted lots of interest recently. From a computational point of view, attractors in a chaotic system can be classified as self-excited and hidden attractors. An attractor is called a self-excited attractor if its attraction basin intersects with any neighborhoods of a stationary state (an equilibrium); otherwise, it is called a hidden attractor. The hidden attractors exist in some special dynamical systems, including ones with one stable equilibrium,[26,27] or without equilibrium,[28,29] or with a line equilibrium (infinite equilibria).[30] It is thought that the number of multi-scroll attractors or multi-wing attractors in the dynamical systems has a close relation with the system equilibria, and the dynamical systems with multi-scroll attractors or multi-wing attractors are commonly constructed by extending saddle-focus equilibrium points with index 2. However, for the systems with multi-scroll hidden attractors or multi-wing hidden attractors, the generating mechanism does not make sense because the systems have no equilibrium.

Most of the dynamical systems with hidden attractors only have one or two attractors, and the dynamical systems with multi-scroll hidden attractors or multi-wing hidden attractors are seldom reported.[31–34] In Ref. [31], Tahir *et al.* constructed a 4D chaotic system which has no equilibrium by applying a state feedback controller to a Lorenz-like system, and the new system has multi-wing hidden attractors. Zhou *et al.*[32] proposed no equilibrium hyperchaotic multi-wing attractors via introducing a memristor into a multi-wing chaotic system. Moreover, multi-scroll hidden attractors were also observed in an improved Sprott A system.[33,34] Inspired by the above references, we wonder are there some dynamical systems that can present both multi-scroll hidden attractors and multi-wing hidden attractors simultaneously? The answer is yes. In this paper, we propose a novel 5D memristive chaotic system. Compared with the systems in the references,[31–34] the novel chaotic system can present either multi-scroll hidden attractors or multi-wing hidden attractors on different phase planes. As the novel chaotic system has no equilibrium, the number of multi-scroll hidden attractors and multi-wing hid-

*Project supported by the National Natural Science Foundation of China (Grant Nos. 51177117 and 51307130).

†Corresponding author. E-mail: huxiaoyucool@163.com

© 2017 Chinese Physical Society and IOP Publishing Ltd

den attractors has nothing to do with the system equilibrium. Particularly, it is sensitive to the transient simulation time and initial values.

The organization of this paper is as follows. In Section 2, the mathematical model is introduced, and some dynamics analysis is carried out in a numerical way. In Section 3, an electronic circuit implementation for the new chaotic system is discussed and analyzed carefully. Section 4 summarizes this paper.

2. Mathematical model and dynamics analysis

2.1. Mathematical model

The memristor is a two-terminal electronic element which was predicted by Chua,[35] and it is also recognized as the fourth fundamental electronic element. For a memristor, the magnetic flux φ between the terminals is a function of the electric charge q that passes through the device. In this paper, a flux controlled one is used, and the nonlinear relation between terminal voltage u and terminal current i is defined as follows:

$$i = W(\varphi)u, \quad \dot{\varphi} = u, \tag{1}$$

where $W(\varphi)$ is an incremental memductance function, and is given by

$$W(\varphi) = h + g\varphi^2. \tag{2}$$

In this paper, we propose a novel dynamical system whose dynamics is described as follows:

$$\begin{cases} \dot{x} = ay, \\ \dot{y} = by - z + c\sin(2\pi dx), \\ \dot{z} = y - ez, \\ \dot{u} = -xy - (g + h\varphi^2)u + k, \\ \dot{\varphi} = u, \end{cases} \tag{3}$$

where a, b, c, d, e, k, g, h are system parameters. The equilibria of Eq. (3) can be obtained by calculating the following equations:

$$\begin{cases} ay = 0, \\ by - z + c\sin(2\pi dx) = 0, \\ y - ez = 0, \\ -xy - (g + h\varphi^2)u + k = 0, \\ u = 0. \end{cases} \tag{4}$$

The parameter k is the key factor that determines the type of solutions.

Case A: when $k = 0$, the equilibria of Eq. (3) are $(n/2d,\ 0,\ 0,\ 0,\ \varphi^*)$, where n is an integer number and φ^* is an arbitrary real constant, which means the equilibria are multiple lines equilibria.

Case B: when $k \neq 0$, obviously, there is no solution for Eq. (4) whatever the system parameters are.

According to the definition of hidden attractors, the attractors of the dynamical system under the condition of either case A or case B are hidden. In this work, we focus on the dynamical system under the condition of case B, and the system parameters are chosen as $a = 0.25$, $b = 0.4$, $c = 2$, $d = 0.5$, $e = 0.5$, $g = 15$, $h = 0.01$, and $k = 0.05$. Dynamics analyses of the new system are presented in the next subsection.

2.2. Dynamics analysis

Obviously, in case B, the new dynamical system has no equilibrium, and any attractors of this system are hidden according to the definition of hidden attractors. When the initial values $(x_0,\ y_0,\ z_0,\ u_0,\ \varphi_0 = 0.2,\ 0,\ 0,\ 0,\ 0.2)$ and transient simulation time $t = 3000$ are selected, the numerical results are shown in Fig. 1. In Fig. 1, 4-scroll hidden attractors and 8 butterfly wing hidden attractors can be observed on the x–y phase plane and y–u phase plane, respectively. The projections on different phase planes show the clear characteristic that all the hidden attractors are solid, which are different from the self-excited attractors.

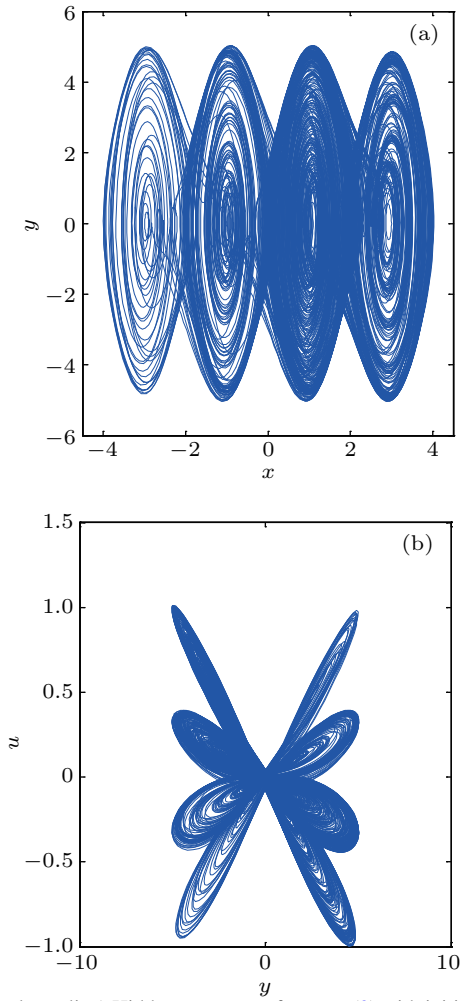


Fig. 1. (color online) Hidden attractors of system (3) with initial values $(x_0,\ y_0,\ z_0,\ u_0,\ \varphi_0 = 0.2,\ 0,\ 0,\ 0,\ 0.2)$, and transient simulation time $t = 3000$ time units: (a) 4 scrolls hidden attractors on the x–y phase plane, (b) 8 butterfly wing hidden attractors on the y–u phase plane.

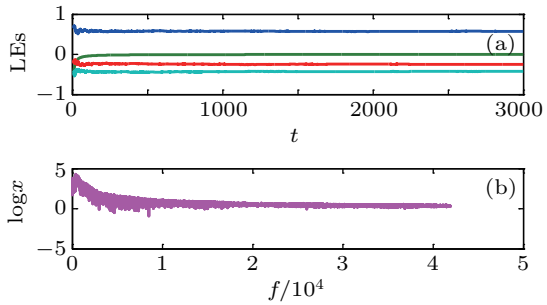


Fig. 2. (color online) Dynamical properties of system (3) with initial values $(x_0,\ y_0,\ z_0,\ u_0,\ \varphi_0 = 0.2,\ 0,\ 0,\ 0,\ 0.2)$, and transient simulation time $t = 3000$ time units: (a) convergence curves of four largest Lyapunov exponents, (b) frequency spectra.

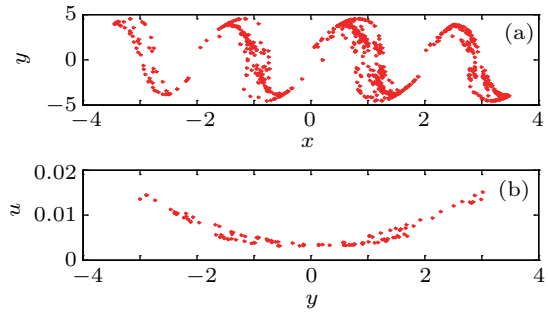


Fig. 3. (color online) Poincare maps of system (3) with initial values $(x_0,\ y_0,\ z_0,\ u_0,\ \varphi_0 = 0.2,\ 0,\ 0,\ 0,\ 0.2)$, and transient simulation time $t = 3000$ time units: (a) Poincare map on the x–y phase plane with $z = 0$; (b) Poincare map on the y–u phase plane with $x = 0$.

According to the chaos theory, Lyapunov exponents measure the exponential rates of divergence or convergence of nearby trajectories of a nonlinear dynamical system in phase space, and one positive Lyapunov exponent indicates that the dynamical system is chaotic. Convergence curves of four largest Lyapunov exponents of system (3) are shown in Fig. 2(a), as the time goes to 3000 time units, there always exists a positive Lyapunov exponent. Frequency spectral state variable x is shown in Fig. 2(b); its spectrum is continuous. Poincaré maps are shown in Fig. 3. The Poincaré map consists of a mess of points on the phase plane. All of the evidence indicates that the system has chaotic characteristics.

2.3. Dynamics dependent on transient simulation time

Extensive numerical simulations confirm that the number of multi-scroll hidden attractors and multi-butterfly wing hidden attractors of the dynamical system is dependent on the transient simulation time. When the initial values are selected as $(x_0,\ y_0,\ z_0,\ u_0,\ \varphi_0 = 0.2,\ 0,\ 0,\ 0,\ 0.2)$, the results of the numerical simulations with different transient times are shown in Fig. 4. As shown in Fig. 4, longer transient simulation time leads to a larger number of multi-scroll or multi- butterfly wing hidden attractors.

The dynamical system generates a different number of multi-scroll hidden attractors and multi-butterfly wing hidden attractors when the transient simulation time changes; this is because the nonlinearity of Eq. (3) is unbound,[10] which is due to the existence of the sine function in Eq. (3). Time series of state variable x are shown in Fig. 5, it is clear that the time series are non-periodic, and the absolute value of state variable x increases as the transient simulation time goes to 8000 time units, which results in a larger number of multi-scroll hidden attractors.

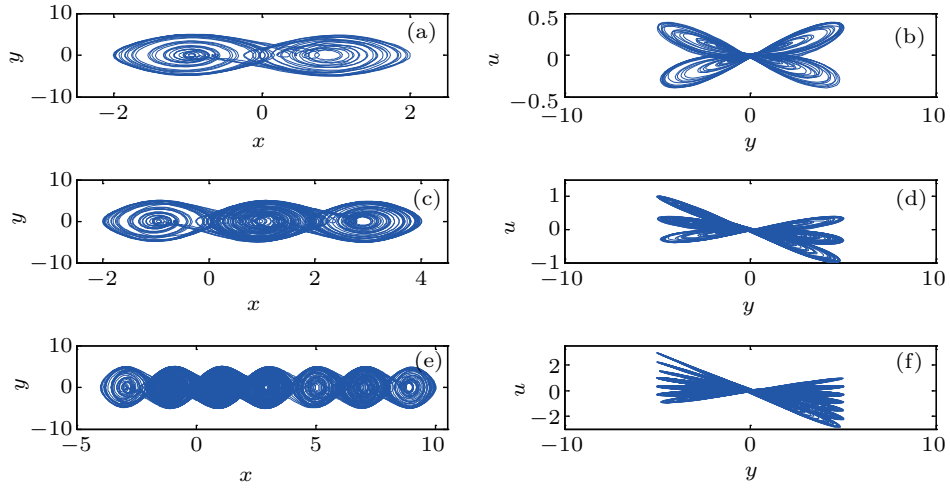


Fig. 4. (color online) Multi-scroll hidden attractors and multi-butterfly wing hidden attractors obtained by setting different transient simulation times on different phase planes, and the initial values are selected as $(x_0,\ y_0,\ z_0,\ u_0,\ \varphi_0 = 0.2,\ 0,\ 0,\ 0,\ 0.2)$: (a), (b) $t = 300$; (c), (d) $t = 1000$; (e), (f) $t = 5000$.

It is inconvenient to apply this kind of attractor in reality; therefore some schemes should be employed to constrain the nonlinearity of the dynamical system. In Refs. [10] and [33], piecewise sine functions were used to avoid the augment of attractors when the transient simulation time went to infinity. Li *et al.*[13] handled the problem through synchronizing two systems and obtained the desired number of attractors. In Ref. [14], Ma *et al.* proposed a simple state feedback controller to constrain the range of state variable x, and the number of multi-scroll attractors could be selected by adjusting two control parameters. In this paper, a state feedback controller which is similar to Ref. [14] is used, and the controlled dy-

namical system can be rewritten as

$$\begin{cases} \dot{x} = ay + f(x), \\ \dot{y} = by - z + c\sin(2\pi dx), \\ \dot{z} = y - ez, \\ \dot{u} = -xy - (g + h\varphi^2)u + k, \\ \dot{\varphi} = u, \end{cases} \tag{5}$$

where $f(x) = -ax(2 - \mathrm{sgn}(x-\alpha) + \mathrm{sgn}(x-\beta))$, α and β are the control parameters, $\alpha < 0 < \beta$, and $\mathrm{sgn}(x)$ is the sign function defined as follows:

$$\mathrm{sgn}(x) = \begin{cases} 1, & x > 0, \\ 0, & x = 0, \\ -1, & x < 0. \end{cases}$$

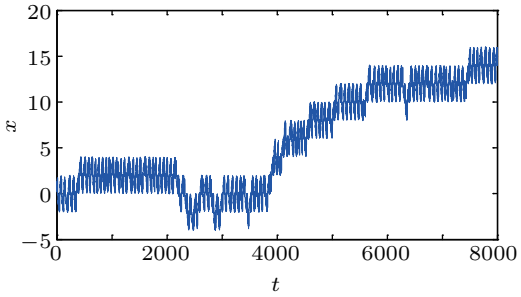


Fig. 5. (color online) Time series of state variable x with initial values and transient simulation time selected as (x_0, y_0, z_0, u_0, φ_0 = 0.2, 0, 0, 0, 0.2) and $t = 8000$ time units.

When the initial values (x_0, y_0, z_0, u_0, $\varphi_0 = 0.2$, 0, 0, 0, 0.2) and transient simulation time $t = 3000$ time units are selected, the uncontrolled system (3) presents 7 scroll hidden attractors and 14 butterfly wing hidden attractors, as shown in Figs. 4(e) and 4(f), respectively. By using the same parameters and setting control parameters $\alpha = -2$ and $\beta = 8$, the numerical simulation results of controlled system (5) are obtained and shown in Fig. 6. In Fig. 6(a), there are 5 scroll hidden attractors on the x–y phase plane, and the value of state variable x is limited in the range (α, β), i.e., (−2, 8). In Fig. 6(b), 10 butterfly wings are obtained on the y–u phase plane. The designed state feedback controller is simple and feasible, and the number of hidden attractors of the dynamical system can be adjusted by only controlling the two parameters.

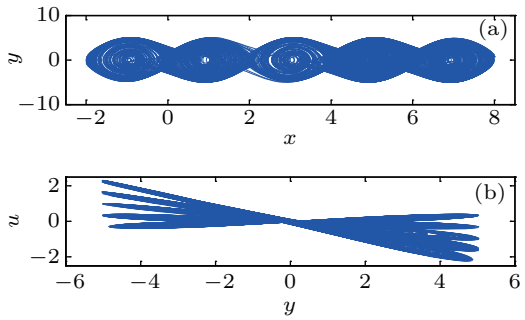


Fig. 6. (color online) Multi-scroll hidden attractors and multi-butterfly wing hidden attractors of the controlled system, the transient simulation time and initial values are selected as $t = 5000$ and (x_0, y_0, z_0, u_0, φ_0 = 0.2, 0, 0, 0, 0.2), and the control parameters are chosen as $\alpha = -2$ and $\beta = 8$: (a) 5 scroll hidden attractors on the x–y phase plane, (b) 10 butterfly wing hidden attractors on the y–u phase plane.

2.4. Dynamics dependent on initial values

As is known to all, the sensitivity to the initial values is a basic characteristic of chaotic systems. Particularly, it is common that the dynamical systems with hidden attractors have the feature of multistability.[36–38] In this subsection,

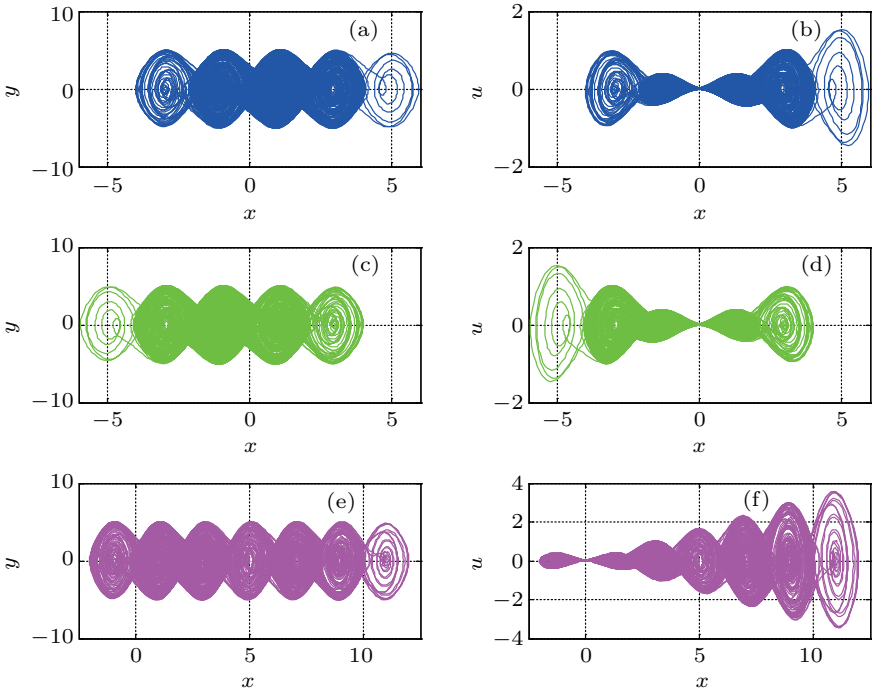


Fig. 7. (color online) Multi-scroll hidden attractors of dynamical system (3) obtained by setting different initial values, and transient simulation time $t = 4000$ time units: (a), (b) (x_0, y_0, z_0, u_0, $\varphi_0 = 0.2$, 0, 0, 0, 0.2); (c), (d) (x_0, y_0, z_0, u_0, $\varphi_0 = -0.2$, 0, 0, 0, 0.2); (e), (f) (x_0, y_0, z_0, u_0, $\varphi_0 = 0.2$, 0, 0, 0, 0.1).

the effects of the initial values on the dynamics of system (3) are studied. Transient simulation time is selected as $t = 4000$ time units, and the numerical simulation results of the dynamical system with different initial values are shown in Fig. 6.

In Figs. 7(a) and 7(b), the initial values of the numerical simulations are chosen as $(x_0, y_0, z_0, u_0, \varphi_0 = 0.2, 0, 0, 0, 0.2)$ and $(x_0, y_0, z_0, u_0, \varphi_0 = -0.2, 0, 0, 0, 0.2)$, respectively, and 5 scroll hidden attractors can be observed on the x–y phase plane and the x–u phase plane. In Fig. 7(c), the initial values $(x_0, y_0, z_0, u_0, \varphi_0 = 0.2, 0, 0, 0, 0.1)$ are selected, and 7 scroll hidden attractors are obtained on the x–y phase plane and x–u phase plane.

In conclusion, besides transient simulation time, the initial values can also affect the dynamics of the system. This dynamical system has the feature of multistability, and multiple hidden attractors coexist on the same phase plane.

3. Electronic circuit implementation

Circuit implementation is a vital procedure for practical applications in reality, and it is also a feasible way to verify the corrections of numerical simulations and theory analysis. Some fundamental analog devices are used in the realization of controlled dynamical system (5), and the whole circuit diagram is shown in Fig. 8. In Fig. 8, OP-07 is used as an operational amplifier, which has saturated voltage $\pm|V_{\rm sat}| = \pm 14.8$ V, and the power supplies for the active device are ± 15 $V_{\rm DC}$.

Based on the mathematical model of system (5), by applying the Kirchhoff circuit laws to the circuit in Fig. 8, the circuit equations can be written as follows:

$$\begin{cases} \dfrac{{\rm d}X}{{\rm d}t} = \dfrac{1}{R_2C_1}Y - \dfrac{1}{R_1C_1}X(V_3 - {\rm sgn}(X - V_1) + {\rm sgn}(X - V_2)), \\ \dfrac{{\rm d}Y}{{\rm d}t} = \dfrac{1}{R_4C_2}Y - \dfrac{1}{R_6C_2}Z + \dfrac{1}{R_5C_2}\sin(m_1X), \\ \dfrac{{\rm d}Z}{{\rm d}t} = \dfrac{1}{R_{12}C_3}Y - \dfrac{1}{R_{11}C_3}z, \\ \dfrac{{\rm d}U}{{\rm d}t} = \dfrac{1}{R_{14}C_4}XY - \left(\dfrac{1}{R_{15}C_4} + \dfrac{1}{R_{16}C_4}\varphi^2\right)U + \dfrac{1}{R_{17}C_4}V_4, \\ \dfrac{{\rm d}\varphi}{{\rm d}t} = -\dfrac{1}{R_{19}C_5}\int U\,{\rm d}t, \end{cases}$$

where state variables X, Y, Z, and U are associated with the voltages across the capacitors C_1, C_2, C_3, and C_4, respectively. State variable φ is associated with the magnetic flux obtained from the output terminal of U_5. m_1 is the gain module,

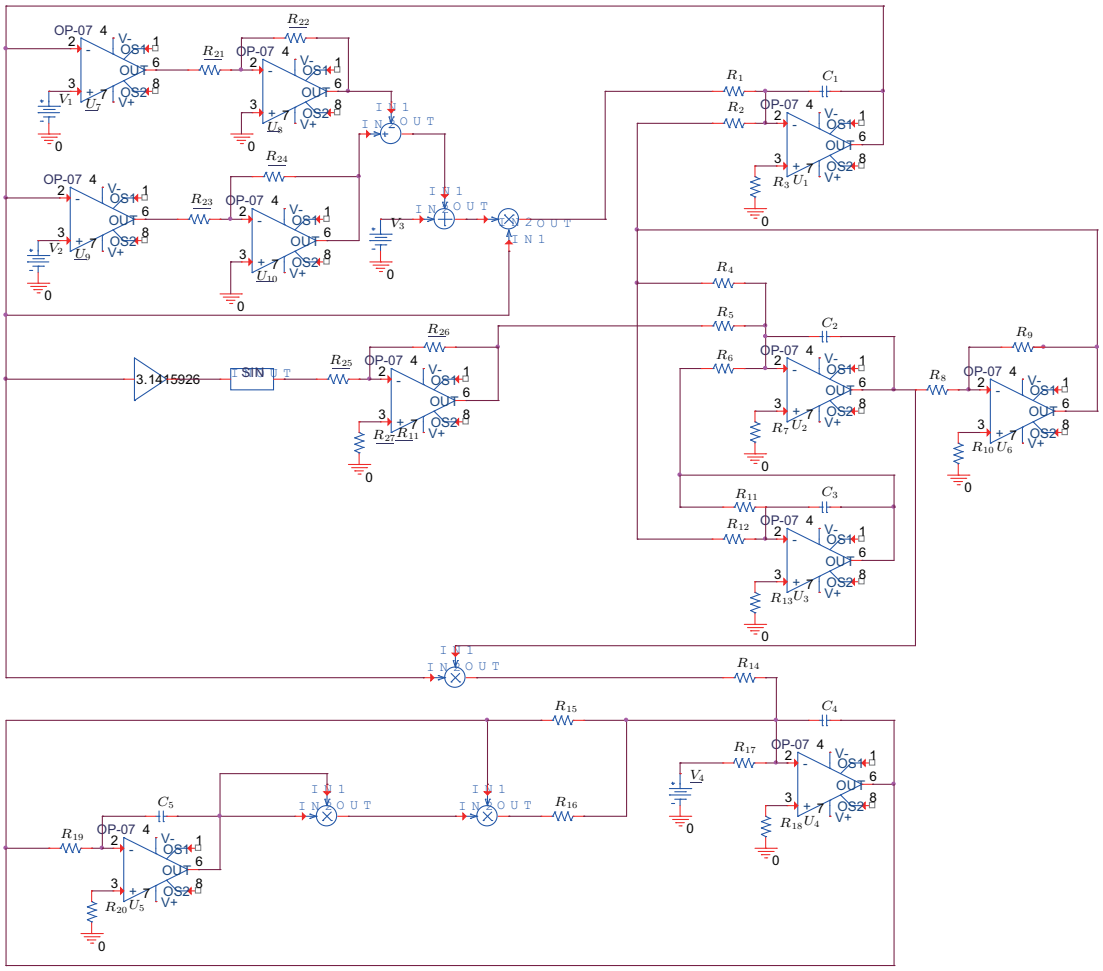


Fig. 8. (color online) Whole circuit implementation of system (5) in Pspice.

and $m_1 = 3.14$. $C_1 = C_2 = C_3 = C_4 = C_5 = 1$ nF, $R_1 = R_2 = 400$ kΩ, $R_4 = 250$ kΩ, $R_5 = 50$ kΩ, $R_6 = 100$ kΩ, $R_8 = R_9 = 100$ kΩ, $R_{11} = 200$ kΩ, $R_{12} = 100$ kΩ, $R_{14} = 100$ kΩ, $R_{15} = 6.67$ kΩ, $R_{16} = 10000$ kΩ, $R_{17} = 1000$ kΩ, $R_{19} = 100$ kΩ, $R_{21} = R_{23} = 14.8$ kΩ, $R_{22} = R_{24} = 1$ kΩ, and $R_{25} = R_{26} = 100$ kΩ. The balance resistors used in the circuit are selected as $R_3 = 200$ kΩ, $R_7 = 29.5$ kΩ, $R_{10} = 50$ kΩ, $R_{13} = 66.7$ kΩ, $R_{18} = 62$ kΩ, $R_{20} = 100$ kΩ, and $R_{27} = 50$ kΩ. The voltage sources $V_3 = 2$ V and $V_4 = -0.5$ V.

The state feedback controller $f(x)$ in system (5) is realized based on the saturated characteristic of operational amplifier OP-07. The circuit of the controller consists of operational amplifiers U_7, U_8, U_9, U_{10}, voltage sources V_1, V_2, V_3, and some accessory circuit elements. The voltage sources V_1 and V_2 are associated with control parameters α and β. By adjusting the voltage sources V_1 and V_2, the desired number of multi-scroll hidden attractors and multi-butterfly wing hidden attractors can be obtained from the circuit. When the voltage sources V_1 and V_2 are set as $V_1 = -2$ V and $V_2 = 8$ V, 5 scroll hidden attractors on the x–y phase plane and 10 butterfly wing hidden attractors on the y–u phase plane can be observed, as shown in Figs. 9 and 10, respectively.

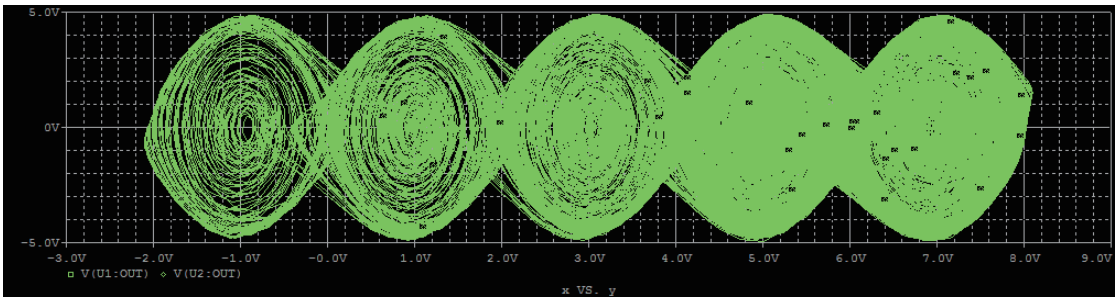


Fig. 9. (color online) 5 scroll hidden attractors of system (5) on the x–y phase plane obtained by setting voltage sources $V_1 = -2$ V and $V_2 = 8$ V, i.e., $\alpha = -2$ and $\beta = 8$.

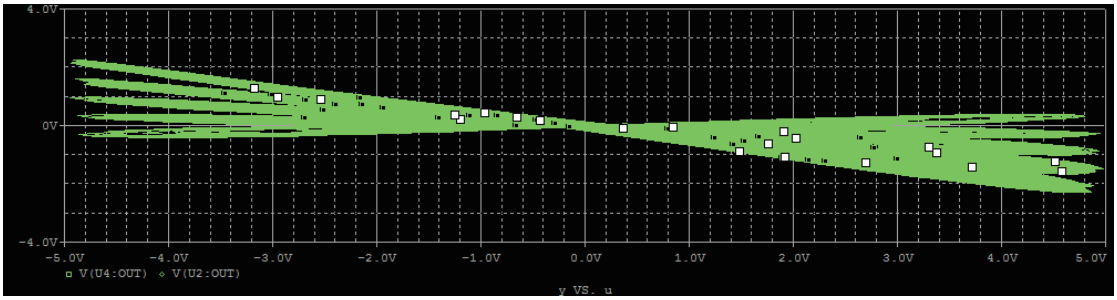


Fig. 10. (color online) 10 butterfly wing hidden attractors of system (5) on the y–u phase plane obtained by setting voltage sources $V_1 = -2$ V and $V_2 = 8$ V, i.e., $\alpha = -2$ and $\beta = 8$.

4. Conclusion

A novel 5D chaotic system is proposed, which has no equilibrium or multiple lines equilibria. When certain system parameters are chosen, multi-scroll hidden attractors and multi-butterfly wing hidden attractors can be observed on different phase planes, and the number of multi-scroll hidden attractors and multi-butterfly wing hidden attractors has nothing to do with the system equilibrium. Extensive numerical simulations confirm that both transient simulation time and initial values have a significant impact on the number of hidden attractors. A state feedback controller is designed and added to the first equation of system (3). The unbound nonlinearity of the dynamical system can be controlled, and state variable x is limited into a desired range. By adjusting only two parameters of the controller, one can obtain the desire number of hidden attractors. The initial values can change the number and position of hidden attractors in phase space, and the effects of the initial values on the dynamics result in multiple hidden attractors coexisting in phase space.

A circuit is designed and implemented in Pspice based on the mathematical model of system (5), from which multi-scroll hidden attractors and multi-butterfly wing hidden attractors can be observed. The results of the circuit experiment have a good agreement with the numerical ones, which validates the circuit. The high complexity and adjustability of multi-scroll hidden attractors and multi-butterfly wing hidden attractors provide a good prospect for chaos-based applications, and the application of this kind of dynamical system will be studied in the near future.

References

[1] Han F, Hu J, Yu X and Wang Y 2007 *Applied Mathematics and Computation* **185** 931

[2] Gámez-Guzmán L, Cruz-Hernández C, López-Gutiérrez R M and García-Guerrero E E 2009 *Commun. Nonlinear Sci. Numer. Simul.* **14** 2765
[3] Ben Slimane N, Bouallegue K and Machhout M 2017 *Nonlinear Dyn.*
[4] Orue A B, Alvarez G, Pastor G, Romera M, Montoya F and Li S 2010 *Commun. Nonlinear Sci. Numer. Simul.* **15** 3471
[5] Yu S, Lü J and Chen G 2007 *Phys. Lett. A* **364** 244
[6] Dadras S and Momeni H R 2009 *Phys. Lett. A* **373** 3637
[7] Bao B, Wang X and Xu J 2010 2010 *International Works hop on Chaos-Fractals Theories and Applications (IWCFTA)* 211
[8] Xu F and Yu P 2010 *Journal of Mathematical Analysis & Applications* **362** 252
[9] Tahir F R, Ali R S, Pham V T, Buscarino A, Frasca M and Fortuna L 2016 *Nonlinear Dyn.* **85** 2665
[10] Tang W K S, Zhong G Q, Chen G and Man K F 2001 *IEEE Transactions on Circuits & Systems I: Fundamental Theory & Applications* **48** 1369
[11] Zhang C and Yu S 2010 *Phys. Lett. A* **374** 3029
[12] Yu S, Lu J, Chen G and Yu X 2011 *IEEE Transactions on Circuits & Systems II: Express Briefs* **58** 314
[13] Li F and Yao C 2016 *Nonlinear Dyn.* **84** 2305
[14] Ma J, Wu X, Chu R and Zhang L 2014 *Nonlinear Dyn.* **76** 1951
[15] Yalçin M E 2007 *Chaos Soliton. Fract.* **34** 1659
[16] Bao B, Zhou G, Xu J and Liu Z 2010 *Int. J. Bifurcation Chaos* **20** 2203
[17] Ahmad W M 2005 *Chaos Soliton. Fract.* **25** 727
[18] Deng W and Lü J 2007 *Phys. Lett. A* **369** 438
[19] Cang S, Wu A, Wang Z, Xue W and Chen Z 2015 *Nonlinear Dyn.* **83** 1987
[20] Zhou L, Wang C and Zhou L 2016 *Nonlinear Dyn.* **85** 2653
[21] Wang C, Xia H and Zhou L 2017 *Int. J. Bifurcation Chaos* **27** 1750091
[22] Zhou L, Wang C and Zhou L 2017 *Int. J. Bifurcation Chaos* **27** 1750027
[23] Dudkowski D, Jafari S, Kapitaniak T, Kuznetsov N V, Leonov G A and Prasad A 2016 *Physics Reports* **637** 1
[24] Leonov G A and Kuznetsov N V 2013 *Int. J. Bifurcation Chaos* **23** 1330002
[25] Kuznetsov N V 2016 *AETA 2015: Recent Advances in Electrical Engineering and Related Sciences* **371** 13
[26] Wang X and Chen G 2012 *Commun. Nonlinear Sci. Numer. Simul.* **17** 1264
[27] Molaie M, Jafari S, Sprott J C and Golpayegani S M R H 2013 *Int. J. Bifurcation Chaos* **23** 1350188
[28] Wei Z 2011 *Phys. Lett. A* **376** 102
[29] Jafari S, Sprott J C and Hashemi Golpayegani S M R 2013 *Phys. Lett. A* **377** 699
[30] Jafari S and Sprott J C 2013 *Chaos Soliton. Fract.* **57** 79
[31] Tahir F R, Jafari S, Pham V T, Volos C and Wang X 2015 *Int. J. Bifurcation Chaos* **25** 1550056
[32] Zhou L, Wang C and Zhou L 2017 *International Journal of Circuit Theory and Applications*
[33] Hu X, Liu C, Liu L, Ni J and Li S 2016 *Nonlinear Dyn.* **86** 1725
[34] Jafari S, Pham V T and Kapitaniak T 2016 *Int. J. Bifurcation Chaos* **26** 1650031
[35] Chua L 1971 *IEEE Transactions on Circuit Theory* **18** 507
[36] Li C and Sprott J C 2014 *Int. J. Bifurcation Chaos* **24** 1450131
[37] Li C and Sprott J C 2014 *Int. J. Bifurcation Chaos* **24** 1450034
[38] Sharma P R, Shrimali M D, Prasad A, Kuznetsov N V and Leonov G A 2015 *The European Physical Journal Special Topics* **224** 1485